Published in IET Electrical Systems in Transportation
Received on 23rd August 2012
Revised on 22nd February 2013
Accepted on 18th March 2013
doi: 10.1049/iet-est.2012.0027

ISSN 2042-9738

Effect of vehicle mass changes on the accuracy of Kalman filter estimation of electric vehicle speed

David Hodgson[1,2], Barrie Charles Mecrow[1], Shady M. Gadoue[1], Howard J. Slater[2], Peter G. Barrass[2], Damian Giaouris[1]

[1]*School of Electrical and Electronic Engineering, Newcastle University, Newcastle Upon Tyne, UK*
[2]*Sevcon Ltd, Gateshead, UK*
E-mail: David.hodgson1@ncl.ac.uk; david.hodgson@sevcon.com

Abstract: The mechanical drivetrain dynamics of electric vehicles can have a detrimental effect on the performance of the vehicle speed controller. It is common for the speed measurement from the motor encoder to be used for the vehicle speed feedback, after taking into account the gear ratio, but it is not valid to assume that motor and vehicle speeds are equal during transient conditions. In this study it is shown how the vehicle driveability can be greatly improved if estimates of vehicle speed and mass are obtained. Estimates of vehicle speed and mass have been realised using a Kalman filter (KF) and a recursive least-squares estimator, and validated with experimental results. The study also shows the importance of finding the most optimal process noise matrix $\boldsymbol{Q}$ for the KF, this has been carried out using a genetic algorithm, with the estimation accuracy then compared with varying vehicle mass.

1 Introduction

Industrial and leisure electric vehicles (EV) ranging from lower cost golf buggies and utility vehicles to higher end airport tow tractors and fork lift trucks all require smooth progressive acceleration, no oscillations in the drivetrain and precise speed control for slow-speed manoeuvres. This response is expected, regardless of load changes and poor mechanical drivetrain components such as gear backlash. These vehicles typically have either a single traction motor driving both wheels on one axle through a fixed ratio differential, or twin traction motors driving left and right wheels, each through their own fixed ratio gearbox.

During steady state, constant torque and load conditions, the motor and vehicle speeds are equal, after taking into account the gear ratio and tyre radius. Whenever the motor torque changes, the drivetrain mechanical dynamics allow the motor speed to initially change much more rapidly than the vehicle speed, which then develops into a damped oscillation of motor speed if the torque change is significant. This affects both the speed feedback and the smoothness of the vehicle's response. Speed feedback is often only available from the motor encoder as most industrial vehicles do not have wheel speed sensors to give vehicle speed. The model of the drivetrain can be compared with that often found in some industrial systems such as rolling mills; where there is a low inertia motor, gearbox with backlash, flexible shaft and a large inertia load.

The objective is to obtain smooth control with parameter independence, which is accomplished by controlling the vehicle speed rather than the motor speed. As vehicle speed is not measured, the use of a Kalman filter (KF) is introduced to estimate the actual vehicle speed, taking into account that vehicle parameters such as mass and tyre stiction can change. The effect of parameter variation on the estimator accuracy is shown and a solution to overcome this using recursive least-squares (RLS) estimation is presented. The use of RLS has previously been shown to be successful for estimating the mass of heavy duty diesel trucks [1]. A simple damping algorithm is also used that aims to reduce the difference in motor and vehicle speed. These concepts have been implemented on a test vehicle, with a marked improvement in vehicle driveability. This paper builds on previous work in [2], adding results detailing the effect of estimator setup on its mass robustness. The proposed estimation algorithm has been shown to have the advantages of being robust to significant mass changes and working over a large speed range. This has allowed the control scheme to improve both the responsiveness and smoothness of the vehicle's response.

The drivetrain oscillations can be limited by simply limiting the rate of change of torque, but this gives a sluggish driving response [3] and will limit the dynamic performance of the speed loop, therefore active damping methods are required. A common solution to damping oscillations is to estimate the gear torque and use this to compensate the torque demand, but some schemes require the wheel speed to be measured [4]. It is possible to use an estimator instead of sensors and it has been shown that improved speed control can be obtained by estimating the speed of the load and the shaft (or gear) torque [5–7], but the effects of the load inertia changing significantly have not been considered, which is common for industrial EVs such as tow tractors that run light or have heavy loads.

© The Institution of Engineering and Technology 2013

Other solutions for improving speed control for a dual inertia model system include model predictive control, which has been compared with standard proportional integral (PI) speed control and PI control using addition estimated feedbacks [6]. The predictive scheme shows dynamic improvement over the standard PI control, and a lower drive shaft stress compared with the PI with multiple feedbacks (PI-based state-space control), but with a much higher calculation time.

Changes in the vehicle mass can significantly change the dynamics of the vehicle and therefore the operation of the estimator and controller. In [8] the effects of load inertia are considered when tuning gains for proportional integral derivative (PID) and linear quadratic controllers, but in this case there is encoder feedback from the load side of the system, rather than estimating all the load side states. Including the load inertia as a state and using the extended Kalman filter (EKF), with only motor side feedback, has been shown to successfully estimate the required states [9]. However, the EKF has to recalculate its matrices at every step, including the Kalman gain matrix, adding a large amount of processing overhead. In this paper, a fixed Kalman gain estimator (often referred to as a steady state KF) has been shown to be capable of estimating the unmeasured load states, even when the load inertia (vehicle mass) is changing, greatly reducing the computational requirement compared with previous work. In the case of significant mass changes or if the KF is not tuned properly, a separate RLS mass estimator has been shown to accurately estimate the mass and when it is found, can update the KF with the correct mass. This recalculation of the KF is only carried out once after the vehicle has started moving, as this is much faster than continuously updating at every time step. RLS has been shown suitable for correcting a KF for low-inertia or low-resolution encoder [10, 11] applications. Although only a single inertia model load is used, with no gearbox and shaft dynamics, this paper applies this theory to a dual inertia model.

The estimation accuracy of the KF requires the correct process noise matrix $\boldsymbol{Q}$ and measurement noise matrix $\boldsymbol{R}$. Two common ways of tuning $\boldsymbol{Q}$ are: innovation-based adaptive estimation, where the innovation sequence is assumed to be white noise if correct $\boldsymbol{Q}$ and $\boldsymbol{R}$ matrices are used; and multiple model adaptive estimation, where multiple models are used on-line and evaluated to find the most accurate solution. Both of these methods, however, have the disadvantage the exact system dynamics are required and they do not always guarantee finding the best $\boldsymbol{Q}$ matrix [12]. It has been decided to use genetic algorithms (GA) for tuning $\boldsymbol{Q}$, as this has been shown to be successful in a similar application [9]. GA also has the advantage that it works well with non-linear stochastic systems, it can avoid local minima and there is no derivative required in the cost function, unlike other optimisation techniques [13]. GA can have the disadvantage that the optimisation process can be very time consuming and take many hours to find the solution, but it is used off-line in this case so this is not an issue.

With regards to the tuning of the $\boldsymbol{Q}$ matrix, previous work only considers the integrated error of the estimated states as being the only performance indicator to optimise. This paper also includes the noise reduction effect of the selected matrix $\boldsymbol{Q}$, as the KF is a balance between reducing noise and being robust to parameter changes or modelling errors. The measurement noise matrix $\boldsymbol{R}$ is calculated directly from the measured signals, motor position and speed, using a similar method to when analysing the KF performance for tuning $\boldsymbol{Q}$. Analysis has been done to compare the estimation performance with: trial and error tuned $\boldsymbol{Q}$, GA tuned $\boldsymbol{Q}$ and also $\boldsymbol{Q}$ tuned from other optimisation techniques, all with and without RLS mass compensation.

This paper is divided into the following sections: Section 2 describes how the model of the vehicle is derived and the approximations that are used to create the two inertia model; Section 3 uses simulations to show how the vehicle driveability can be improved using vehicle speed feedback; Section 4 describes how vehicle speed can be estimated using KF and gives its experimental results; the effect of mass changes on the estimator is considered in Section 5 and the estimation of vehicle mass using RLS is tested; and finally in the last Section 6 a method for tuning the KF noise matrix using GA is shown, and the estimator robustness to mass changes is compared with the trial and error method used in Sections 4 and 5.

2 Vehicle model

A common drivetrain arrangement for EVs consists of a single AC traction motor, connected directly to a fixed ratio differential, driving either the front or rear wheels. This along with the rest of the vehicle dynamics can be simplified into a two mass rotating model, shown in Fig. 1. The model aims to include all the key vehicle components that have the greatest effect on the vehicle driveability, such as the gear backlash and the drivetrain flexibility, while making assumptions about others such as the tyre rotational stiffness being comparatively high it can be ignored, avoiding the requirement for a three inertia model. The left and right dynamics are lumped together as only straight line driving will be considered.

Drive shaft inertia (J_s) is referenced to the vehicle side of the tyre radius, giving an equivalent vehicle mass increase for shaft inertia (m_{axle}). The losses within the drivetrain are modelled as two speed dependant friction terms, for both the motor (b_m) and vehicle side of the gearbox (b_v).

2.1 Vehicle losses

The forces acting on the vehicle itself are rolling resistance of the tyres (1), aerodynamic drag (2) and gradient force (3). The sgn term in the equation is to ensure that the forces always oppose the direction of travel. Gradients have been ignored for this paper as additional sensors would be required in order to include its effect

$$F_{\text{roll}} = -\left(C_0 + C_1 v_{\text{v}} + C_2 v_{\text{v}}^2\right) m_{\text{v}} g \,\text{sgn}\left(v_{\text{v}}\right) \tag{1}$$

$$F_{\text{drag}} = C_{\text{d}} A_{\text{v}} \rho v_{\text{v}}^2 \,\text{sgn}\left(v_{\text{v}}\right) \tag{2}$$

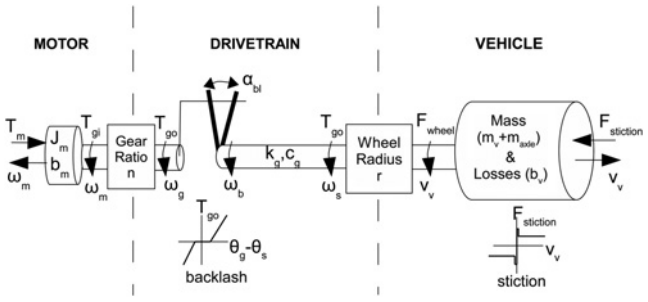

Fig. 1 *Two inertia vehicle drivetrain model*

© The Institution of Engineering and Technology 2013

doi: 10.1049/iet-est.2012.0027

$$F_{\text{grad}} = m_{\text{v}} g \sin(\theta_{\text{road}}) \tag{3}$$

The forces dependant on the square of vehicle speed, mainly aerodynamic drag, have to be linearised to be included within the linear vehicle model: they are then represented within the term b_{v}. This is a valid approximation because of the fact that the vehicles mainly operate at lower speeds, before the speed-squared term dominates the losses. At the operating point chosen of 1500 rpm (2.75 m s^{-1}), the speed square losses only make up 4% of the total mechanical losses.

Rolling resistance includes a non-speed dependant term C_0, often referred to as tyre stiction. This is a significant force acting on the vehicle at slow speeds and cannot be ignored or easily linearised: it makes up the majority of the losses acting upon the vehicle, 56% of losses at 1500 rpm. This is represented as a system input to the vehicle side of the model. The stiction is 40% higher when the vehicle is stationary than when it is moving, because of the extra force required to start the vehicle moving.

2.2 Gear backlash

It is common for gearboxes to have a few degrees of play between the gears, leading to a brief disconnect between its input and output mainly during torque reversals. For the vehicle tested, there was around 30° on the motor side, as it is increased in size by the gear ratio. Gear backlash can be linearised by allowing the vehicle model to operate in two linear modes: contact (co) and backlash (bl). When in contact mode the backlash can effectively be ignored apart from a small fixed angle offset, θ_{bl}, in the differential equation, which is equal to half of the backlash size. When in backlash mode there is no connection between the two rotating masses of the model, motor and vehicle. It is determined to be in this mode when the angle offset between motor and vehicle is less than half the total backlash angle or because of the axle damping, a large speed difference can also trigger this mode before the axle twist has fully unwound; see (4) [14, 15]

$$\text{in backlash} = \text{IF}\left|\left(\frac{\omega_{\text{m}}}{n} - \frac{v_{\text{v}}}{r} - \omega_{\text{bl}}\right)\left(\frac{c_g}{k_g}\right) + \left(\frac{\theta_{\text{m}}}{n} - \frac{d_{\text{v}}}{r}\right)\right| < \left(\frac{\alpha_{\text{bl}}}{2}\right) \tag{4}$$

2.3 Test vehicle parameters

Table 1 contains the parameters of the test vehicle used for the simulation and experimental work.

2.4 Vehicle differential equations

The differentials (5)–(10) describe the vehicle model shown in Fig. 1, which operates in two linear modes: contact and backlash. The states are motor position (θ_{m}) and speed (ω_{m}), vehicle distance (d_{v}) and speed (v_{v}) and the position within the backlash (θ_{bl}) and which is equal to ($\theta_g - \theta_{\text{b}}$); see Fig. 1.

Contact mode

$$\frac{\text{d}}{\text{d}t}\omega_{\text{m}} = \left(\frac{d_{\text{v}}}{nr} - \frac{\theta_{\text{m}}}{n^2} + \frac{\theta_{\text{bl}}}{n}\right)\left(\frac{k_g}{J_{\text{m}}}\right) + \left(\frac{v_{\text{v}}}{nr} - \frac{\omega_{\text{m}}}{n^2}\right)\left(\frac{c_g}{J_{\text{m}}}\right) - \left(\frac{\omega_{\text{m}} b_{\text{m}}}{J_{\text{m}}}\right) + \left(\frac{T_{\text{m}}}{J_{\text{m}}}\right) \tag{5}$$

Table 1 Vehicle parameters

Symbol name	Value	Units
J_{m}	motor inertia	0.003 kg m^2
b_{m}	motor friction	9×10^{-4} Nm/rad
n	gear ratio	12.28
α_{bl}	backlash size (after ratio)	0.0398 rads
k_g	axle/gear stiffness	9000 Nm/rad
c_g	axle/gear damping	25 Nm/rad s^{-1}
r	tyre radius	0.215
b_{v}	vehicle friction	18.825 Nm/s
$C_0.g$	stiction coefficient	0.288 N/kg
J_{axle}	axle inertia	0.02 kg m^2
$m_{\text{axleinertia}}$	axle inertia equivalent mass	71 kg
m_{v}	unloaded mass (including driver)	483 kg
m_{load}	load mass added	200 kg
T_{pk}	peak motor torque	50 Nm

$$\frac{\text{d}}{\text{d}t}v_{\text{v}} = \left(\frac{\theta_{\text{m}}}{nr} - \frac{d_{\text{v}}}{r^2} - \frac{\theta_{\text{bl}}}{r}\right)\left(\frac{k_g}{m_{\text{v}}}\right) + \left(\frac{\omega_{\text{m}}}{nr} - \frac{v_{\text{v}}}{r^2}\right)\left(\frac{c_g}{m_{\text{v}}}\right) - \left(\frac{v_{\text{v}} b_{\text{v}}}{m_{\text{v}}}\right) - \left(\frac{F_{\text{stiction}}}{m_{\text{v}}}\right) \tag{6}$$

$$\frac{\text{d}}{\text{d}t}\theta_{\text{bl}} = 0 \tag{7}$$

Backlash mode

$$\frac{\text{d}}{\text{d}t}\omega_{\text{m}} = -\left(\frac{\omega_{\text{m}} b_{\text{m}}}{J_{\text{m}}}\right) + \left(\frac{T_{\text{m}}}{J_{\text{m}}}\right) \tag{8}$$

$$\frac{\text{d}}{\text{d}t}v_{\text{v}} = -\left(\frac{v_{\text{v}} b_{\text{v}}}{m_{\text{v}}}\right) - \left(\frac{F_{\text{stiction}}}{m_{\text{v}}}\right) \tag{9}$$

$$\frac{\text{d}}{\text{d}t}\theta_{\text{bl}} = \left(\frac{\theta_{\text{m}}}{n} - \frac{d_{\text{v}}}{r} - \theta_{\text{bl}}\right)\left(\frac{k_g}{c_g}\right) + \left(\frac{\omega_{\text{m}}}{n}\right) - \left(\frac{v_{\text{v}}}{r}\right) \tag{10}$$

3 Driveability improvement using vehicle speed feedback

The speed control for an industrial EV generally uses speed feedback from the motor encoder, as the sensor is already present for AC motor flux vector control. PI control is used as it can easily be manually tuned to provide satisfactory performance, Fig. 2. Issues arise from the fact that the gains have to be detuned to maintain stability, because of the transient error when using the motor speed feedback to measure vehicle speed and the fact this signal is prone to oscillation. The oscillation in motor speed directly affects the smoothness of the vehicle acceleration. The simulation results in Figs. 2–5 show the vehicle response when applying a speed demand with a fixed acceleration rate of 1000 rpm/s up to a speed of 1500 rpm, and then decelerating at the same rate after 2 s at a fixed speed (1500 rpm). The acceleration rate is ramped down when approaching the target speed to help prevent overshoot. The demands have been plotted in Fig. 2 only.

In Fig. 2, although the response is smooth, the acceleration never reaches the desired rate of 1000 rpm/s for a constant time; the acceleration should be steady between 0 and 1.5 s. This would give the vehicle a sluggish response that will deteriorate when the vehicle is loaded.

© The Institution of Engineering and Technology 2013

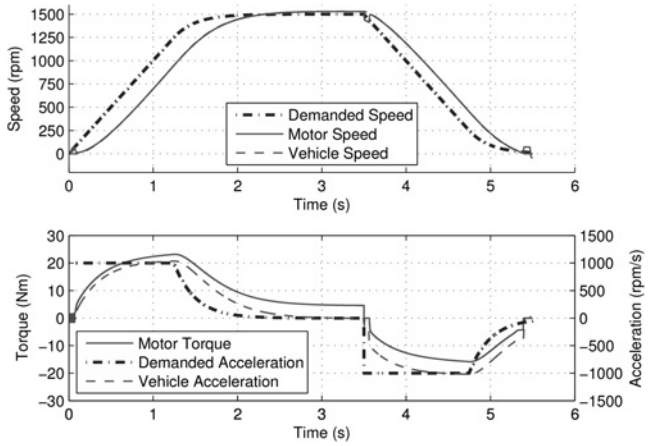

Fig. 2 *Simulation of speed response with motor speed feedback*

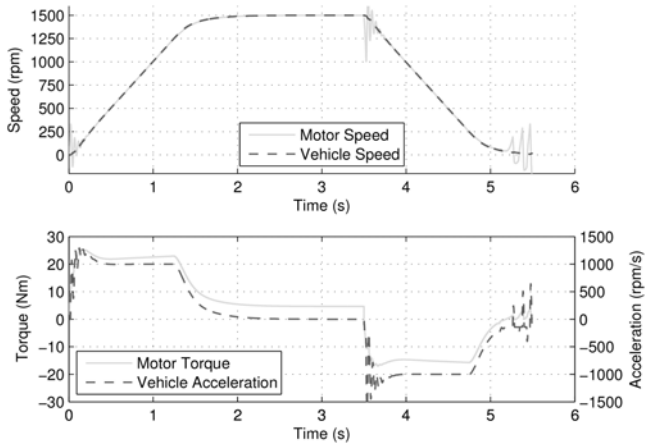

Fig. 3 *Simulation of speed response with vehicle speed feedback*

It has been proposed that improved performance can be obtained through using the actual measured vehicle speed as speed feedback, Fig. 3. Much higher speed gains can be used as the feedback is no longer affected by the motor and drivetrain dynamics. This gives much tighter control of the vehicle speed, and therefore acceleration. It also allows for the control to now include the differential term on speed error (PID controller); previously not possible because of noise on the speed feedback.

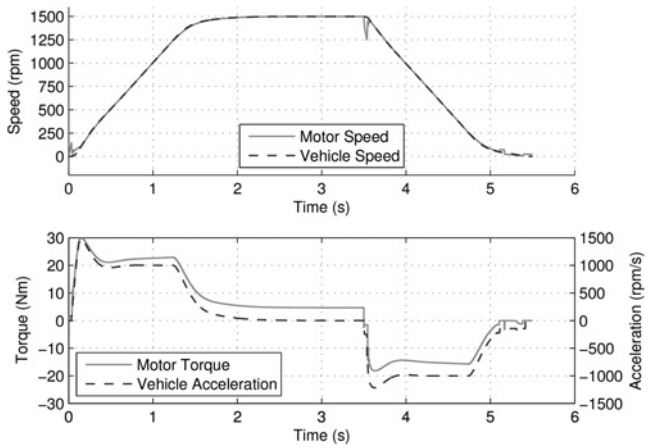

Fig. 4 *Simulation of speed response with vehicle speed feedback and compensator*

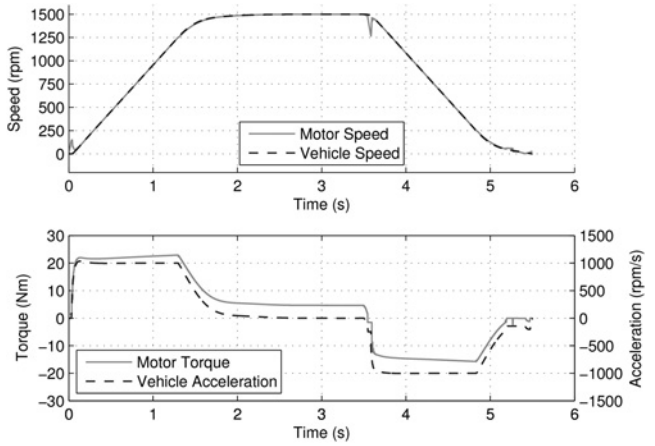

Fig. 5 *Simulation of speed response after implementing all the proposed changes*

Some consideration now needs to be taken to the fact that larger gains will lead to faster torque changes and therefore more oscillation in the drivetrain, see Fig. 3. A simple proportional compensator is introduced that reduces this significantly. The compensator tries to control the motor speed to be equal to the vehicle speed, Fig. 4. This also has the advantage that during the backlash traversal, the torque demand is limited as the motor speed differs greatly from the vehicle speed, the compensator therefore acts to smooth the transition when the gear cogs impact.

This gives a good speed response as it follows the desired speed demand closely, but the acceleration now has an initial disturbance (overshoot) before settling on the steady state value. This will be felt by the driver as a jerk in the vehicle's response. It is caused by the actual vehicle speed lagging behind the demand while going through the backlash, as the motor output torque has no effect on the vehicle during this time because of the disconnect. Then, when in contact mode, the tightly controlled speed loop closes the error quickly.

To improve the response further some modifications to the speed control have been proposed. These are

- Initialising the integrator to be equal to the calculated required torque from the demanded acceleration and vehicle mass – removes the delay of waiting for the integrator to wind up, giving instant acceleration
- Resetting the speed demand to the actual vehicle speed when exiting the backlash mode – prevents the speed loop from having a large error when the backlash closes

It is now possible to obtain a very accurately controlled speed response, but with the acceleration remaining level, Fig. 5. This will give the vehicle driveability a feel of being very responsive and accurate, but smooth in its acceleration.

4 Vehicle speed estimator

The previous section showed the improvement in driveability created if vehicle speed was available, but it is not desirable to add any additional sensors. Kalman filtering is often used to estimate unmeasured states where the feedback signal is subject to noise. It uses a correction based on the measured states, in this case motor position and motor speed, to compensate for parameter uncertainty or model approximation [16].

© The Institution of Engineering and Technology 2013

doi: 10.1049/iet-est.2012.0027

The state space model of the vehicle is shown below [14], these are all converted to their discrete equivalent for calculation in real time with a sample time of 1 ms. This sample rate is chosen as a compromise between the processing requirement and to accurately estimate the fast changing backlash dynamics. It can be clearly seen that during the backlash mode that the motor and vehicle are only affected by their own inputs and friction terms

$$A_{\mathrm{co}} = \begin{pmatrix} 0 & 1 & 0 & 0 & 0 \\ -\dfrac{k_g}{J_{\mathrm{m}}n^2} & -\dfrac{b_{\mathrm{m}} + {}^{c_g}/_{n^2}}{J_{\mathrm{m}}} & \dfrac{k_g}{J_{\mathrm{m}}nr} & \dfrac{c_g}{J_{\mathrm{m}}nr} & \dfrac{k_g}{J_{\mathrm{m}}n} \\ 0 & 0 & 0 & 1 & 0 \\ \dfrac{k_g}{m_{\mathrm{v}}nr} & \dfrac{c_g}{m_{\mathrm{v}}nr} & -\dfrac{k_g}{m_{\mathrm{v}}r^2} & -\dfrac{b_{\mathrm{v}} + {}^{c_g}/_{r^2}}{m_{\mathrm{v}}} & -\dfrac{k_g}{m_{\mathrm{v}}r} \\ 0 & 0 & 0 & 0 & 0 \end{pmatrix} \tag{11}$$

$$A_{\mathrm{bl}} = \begin{pmatrix} 0 & 1 & 0 & 0 & 0 \\ 0 & -\dfrac{b_{\mathrm{m}}}{J_{\mathrm{m}}} & 0 & 0 & 0 \\ 0 & 0 & 0 & 1 & 0 \\ 0 & 0 & 0 & -\dfrac{b_{\mathrm{v}}}{m_{\mathrm{v}}} & 0 \\ \dfrac{k_g}{c_g n} & \dfrac{1}{n} & -\dfrac{k_g}{c_g r} & -\dfrac{1}{r} & -\dfrac{k_g}{c_g} \end{pmatrix} \tag{12}$$

$$B_{\mathrm{co}} = B_{\mathrm{bl}} = \begin{pmatrix} 0 & 0 \\ \dfrac{1}{J_{\mathrm{m}}} & 0 \\ 0 & 0 \\ 0 & \dfrac{1}{m_{\mathrm{v}}} \\ 0 & 0 \end{pmatrix} \tag{13}$$

where the states are θ_{m}, ω_{m}, d_{v}, v_{v} and θ_{bl}, the inputs are T_{m} and F_{stiction} and the measured states are θ_{m} and ω_{m}.

4.1 Determining the noise matrices

The KF requires information on the process and measurement noises of the system. The measurement noise covariance R_{co} (14) can be measured from recorded data of the motor encoder; by separating the noise from the signal and measuring the noise variance. However, obtaining the process noise Q_{co} (15) is less well defined and cannot be directly calculated or measured. A trial and error method has been used to generate suitable values for $\boldsymbol{Q}$ initially. Only diagonal entries are used as they have the most significant effect on the operation of the filter

$$R_{\mathrm{co}} = \begin{pmatrix} R_1 & 0 \\ 0 & R_2 \end{pmatrix} \tag{14}$$

$$Q_{\mathrm{co}} = \begin{pmatrix} Q_1 & 0 & 0 & 0 & 0 \\ 0 & Q_2 & 0 & 0 & 0 \\ 0 & 0 & Q_3 & 0 & 0 \\ 0 & 0 & 0 & Q_4 & 0 \\ 0 & 0 & 0 & 0 & Q_5 \end{pmatrix} \tag{15}$$

To separate the noise from the time-varying signal a number of steps are applied to the data, see Fig. 6. In this application the signals are all quite slow moving vehicle speeds, which are quite low frequency, they are significantly different from that of the noise making it easier to separate the two signals. For the first stage the signal is passed through a second-order low-pass filter with a cut-off of about 6.5 Hz, this filtered signal is then subtracted from the shifted (by approximately the same lag as that of the filter) unfiltered signal. The second stage involves a scond-order high-pass filter with a cut-off of 10 Hz, therefore leaving just the noise signal. The variance of the noise signal can be measured directly in MATLAB and used for determining the $\boldsymbol{R}$ matrix.

4.2 Fixed gain estimator

The KF algorithm includes a large number of matrix multiplications, which increases greatly with the number of states estimated and also the number of measured states. It is required to be implemented on a microcontroller (Texas Instruments TMS320C2811), which also performs numerous other tasks such as the motor control. In order to reduce the computational requirement to a minimum, a fixed Kalman gain is used. The gain can be calculated offline through solving the Riccati equation [17], provided the matrices $\boldsymbol{A}_{\mathrm{d}}$, $\boldsymbol{C}_{\mathrm{d}}$, $\boldsymbol{Q}$ and $\boldsymbol{R}$ remain constant and are known.

The model described in Section 2 suggests that gear backlash can be modelled with two linear modes [14]: switching between these modes online leads to a non-smooth system. This would normally be an issue for the KF and lead to instabilities, but as the Kalman gain is fixed this is less of an issue. During backlash mode the system is not observable or controllable; because of the disconnect between the motor and vehicle, there is only feedback and controllable inputs on the motor side. As this only occurs for very short intervals the Kalman gain is set to zero and the estimator operates on an open loop basis. See (16), (17) for the KF equations used [16]

$$x_k = \left(I - K_{d\_\mathrm{co}}C_d\right)\left(A_{d\_\mathrm{co}}x_{k-1} + B_d u_{k-1}\right) + K_{d\_\mathrm{co}}y_k \tag{16}$$

$$x_k = A_{d\_\mathrm{bl}}x_{k-1} + B_d u_{k-1} \tag{17}$$

4.3 Estimator sample rate different from feedback rate

The encoder is used to generate the speed feedback every 5 ms. The test vehicle is fitted with a hall sensor encoder which has a state transition 6 times every electrical rotation or 24 (as the motor has four-pole pairs) every mechanical rotation. Therefore it is not possible to calculate a new speed at a faster rate than 5 ms. The speed is then integrated to give the estimator the position feedback, as absolute position is not required.

The drivetrain system has fast changing backlash dynamics that requires the estimator to run at least 1 ms to correctly estimate the transition into and out of backlash mode. This

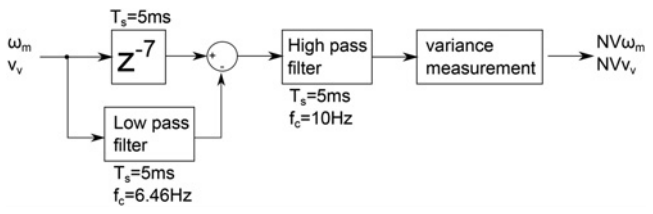

Fig. 6 *Diagram showing how the noise is extracted from the signal*

© The Institution of Engineering and Technology 2013

means that the correction part of the estimator runs five times slower (5 ms) than the state propagation part, see Fig. 9. The Kalman gain is therefore calculated assuming a 5 ms version of $\boldsymbol{A}_{\mathrm{d}}$ and $\boldsymbol{B}_{\mathrm{d}}$, the correction part is divided by 5, so it can be applied over the next five iterations of the estimator, every 1 ms. This also allows the PI speed controller to run at a faster rate than the feedback, therefore increasing its bandwidth.

4.4 Experimental speed estimation results

The speed estimator has been implemented on the test vehicle and the results of this are shown in Fig. 7. When all the vehicle parameters are known it is possible to accurately estimate the vehicle speed. This assumes that the vehicle parameters are not time varying; whereas variables such as tyre rolling resistance and the vehicle mass are likely to change when the vehicle is used, with changing loads and tyre temperature. The variable with the most significant effect is vehicle mass and it is considered in the following two Sections 5 and 6.

5 Mass changes

5.1 Effect of mass change on speed estimator performance

It is common for industrial vehicles to carry or tow large heavy loads: these can be greater than the unloaded mass of the vehicle and therefore this change has a significant impact on the vehicle's response. As there is no feedback from the vehicle side of the system, significant errors in vehicle mass will cause the estimated vehicle speed to drift away from the actual. Feedback is unable to correct this during acceleration, see Fig. 8.

5.2 Mass estimator

The EKF is often used for estimation for time varying non-linear systems, it does however require a large amount of computational time. A simpler method has been proposed using an RLS parameter estimator to track the errors in mass caused by the vehicle being loaded. As mass can only change when the vehicle is stationary, only a single estimate of mass is required as soon as possible after the vehicle has started to move.

A number of assumptions have been used for the mass estimation, such as using motor speed feedback to give vehicle acceleration. This is an issue because of the noise content of the signal and the fact that motor speed is not equal to vehicle speed during transients, especially the case when the vehicle starts to move. This has been solved through using a pre-filter on both the input signals (motor torque and acceleration) to the RLS, a 10 Hz second-order Butterworth low-pass filter which removes most of the noise [18]. The delay of the pre-filter is tolerable as the mass estimate is not used continually in real time to update the KF. Only a single value of mass is selected and used based on the following criteria: the rate of change of the mass estimate is <10 kg for each iteration of the RLS for 20 consecutive samples. This selects the mass value when the estimate has levelled off and reached the correct value.

The entire vehicle dynamics have now been simplified in (18) J_{total} is the entire system inertia, including the vehicle mass and drivetrain inertias, all referenced to the motor. The inertia is then converted to equivalent vehicle mass using (19). As stiction is dependent on the vehicle mass, on every iteration of the RLS algorithm the stiction term is updated, depending on the previous mass estimate (20). This allows both stiction and mass changes to be found while only having one parameter being estimated, meaning all vectors and matrices in the algorithm are 1×1. It does although rely on the stiction remaining proportional to mass across the full vehicle operating load and speed range

$$T_{\mathrm{m}} - T_{\mathrm{stiction}} - \omega_{\mathrm{m}}.b_{\mathrm{total}} = \left(\frac{1}{J_{\mathrm{total}}}\right)\frac{\mathrm{d}\omega_{\mathrm{m}}}{\mathrm{d}t} \tag{18}$$

$$m_{\mathrm{total}} = m_{\mathrm{v}} + m_{\mathrm{load}} = \left(J_{\mathrm{total}} - J_{\mathrm{axle}}\right)\left(\frac{n^2}{r^2}\right) \tag{19}$$

$$T_{\mathrm{stiction}} = \left(m_{\mathrm{v}} + m_{\mathrm{load}}\right)gC_0\left(\frac{r}{n}\right) \tag{20}$$

The RLS algorithm used is shown in (21)–(23) [16] it operates at a sample rate of 5 ms. A fixed forgetting factor $\boldsymbol{R}$ of 0.98 is used, F_k is the motor torque, Θ_k is $1/J_{\mathrm{total}}$ and

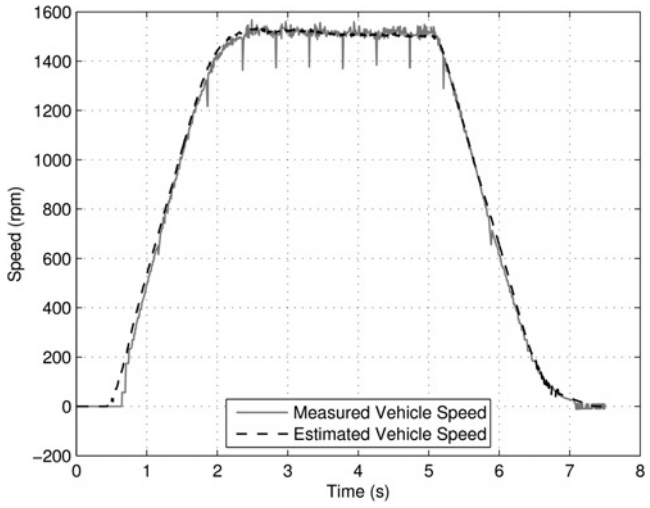

Fig. 7 *Experimental results of speed estimator*

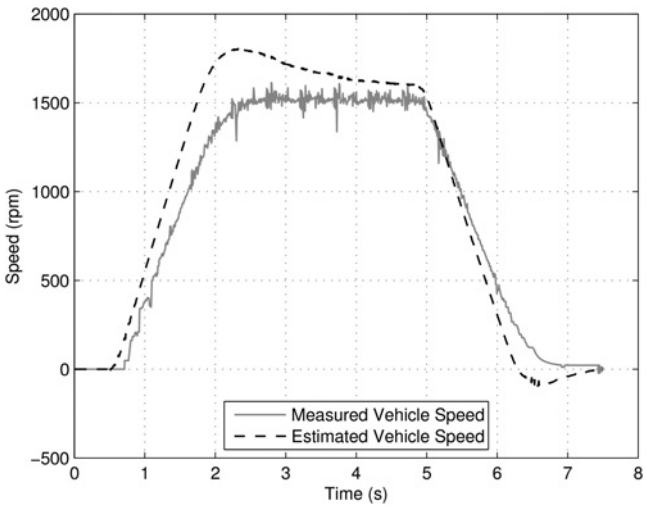

Fig. 8 *Experimental results of speed estimation with 200 kg mass increase from 483 kg unloaded*

© The Institution of Engineering and Technology 2013

doi: 10.1049/iet-est.2012.0027

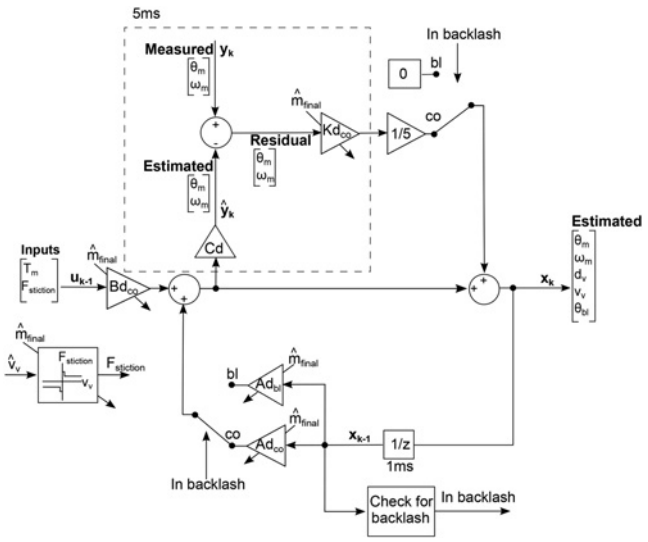

Fig. 9 *Updated KF with mass input and in backlash switch*

Y_k is the measured motor acceleration

$$K_k = P_{k-1}F_k^T\left(F_kP_{k-1}F_k^T + R\right)^{-1} \tag{21}$$

$$\Theta_k = \Theta_{k-1} + K_k\left(Y_k - F_k\Theta_{k-1}\right) \tag{22}$$

$$P_k = R_{k-1}\left(I - K_kF_k\right)P_{k-1} \tag{23}$$

As mass should not change when the vehicle is moving, a single estimate of mass is required as soon as possible after the vehicle has started to move. Fig. 11 shows that it takes about 500 ms for the new vehicle mass to be determined, the mass estimate is obtained at 1.2 seconds after the vehicle starts to move around 0.7 seconds. In this case a value of 709 kg is obtained: vehicle 483 kg, load 200 kg and estimation error 26 kg, the axle and motor inertia equivalent of 71 kg has already been removed from this figure. After the vehicle has stopped and remained stationary for a specified time (couple of seconds), the mass estimate can be reset to the unloaded value, as it can no longer be assumed that the vehicle is still loaded.

5.3 Corrected speed estimator

With the knowledge of the correct mass the speed estimator now needs to be corrected, although up until the mass estimate is found, the unloaded (incorrect) vehicle mass has to be used. For this system, changes in mass leads to a change in the discrete matrices ($\boldsymbol{A}_{\mathrm{d\_co}}$, $\boldsymbol{A}_{\mathrm{d\_bl}}$, $\boldsymbol{B}_{\mathrm{d\_co}}$ and $\boldsymbol{K}_{\mathrm{d\_co}}$). This change is inversely proportional to the change in mass, allowing them to be quickly recalculated. The Jacobian matrices determining the change with mass: $\delta\boldsymbol{A}_{d\_co}/\delta(1/m_{\mathrm{load}})$, $\delta\boldsymbol{A}_{d\_bl}/\delta(1/m_{\mathrm{load}})$, $\delta\boldsymbol{B}_{d}/\delta(1/m_{\mathrm{load}})$ and $\delta\boldsymbol{K}_{d\_co}/\delta(1/m_{\mathrm{load}})$, are calculated offline so that just one multiplication is needed for each entry in the matrices when the new mass is obtained. Fig. 9 shows the KF and highlights which matrices are corrected with mass, the switches are to indicate the transition between contact and backlash mode. The $\boldsymbol{B}_{\mathrm{d\_co}}$ matrix is not switched with backlash, and the contact mode version is always used. There will be a slight difference between its contact and backlash version after it has been converted to its discrete form, it is dependant on the $\boldsymbol{A}_{\mathrm{d}}$ matrix. This was found to be insignificant and so has been ignored to reduce the required storage in the micro controller. The entire speed and mass estimation algorithm takes around 22 µs to execute on average every 1 ms iteration.

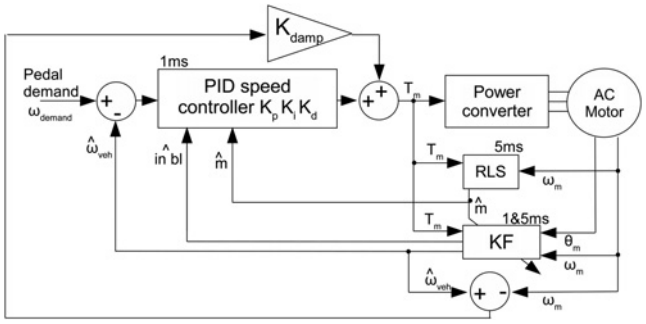

Fig. 10 *Complete system*

The overall system shown in Fig. 10 includes all the proposed solutions in the previous sections of this paper. The RLS mass estimator (Section 5) gives an estimate of mass that is used for correcting the KF and stiction calculation, along with initialising the PID speed loop integrator when there is an acceleration demand change (Section 3). The KF (Section 4) estimates the vehicle speed that is used by the speed controller and the damping algorithm. The in backlash indication is also used to improve the discontinuity in acceleration caused by traversing the backlash (Section 3).

In Fig. 11 the vehicle speed estimation now tracks the measured speed more accurately with a steady state error of about 30 rpm (2%), this is after an extra load mass of 200 kg is added to the vehicle.

6 Tuning the process noise matrix

The process noise matrix $\boldsymbol{Q}$ has a strong influence on the performance of the KF, as it describes the accuracy of the model and so controls the balance between noise reduction and estimation error.

6.1 Cost function

The performance of the estimator is ranked depending upon the per unit (PU) error of the motor speed (24) and vehicle

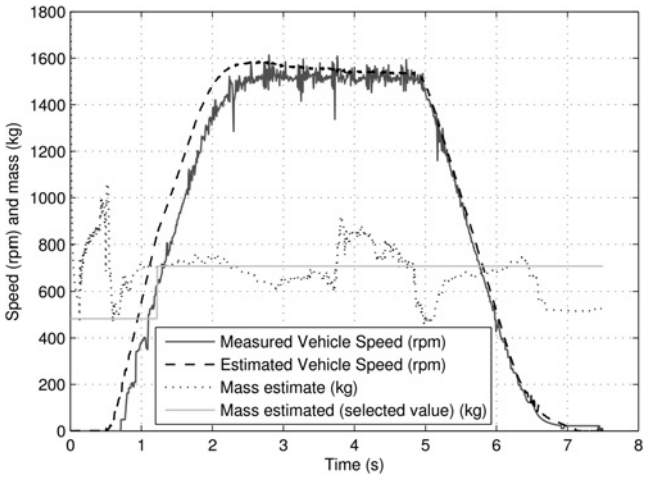

Fig. 11 *Experimental results of speed estimator response with 200 kg load mass*

© The Institution of Engineering and Technology 2013

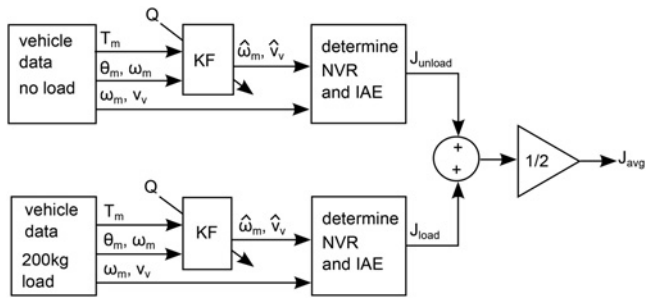

Fig. 12 *Diagram showing how the potential* ***Q*** *values are simultaneously evaluated on two sets of measured vehicle data*

speed (25) estimation, and also the noise reduction of the simulated signals compared with the measured ones (26), (27). It is quite common to only try to minimise the estimation error only [19, 20], but in this case the noise is also considered. This has been carried out using the same method as used for determining matrix ***R***; by extracting the noise from the signal (measured and estimated) using high pass filtering and then measuring the variance of this noise signal.

It is desirable to find values for ***Q*** that are robust to changes in the vehicle's mass; so that accurate vehicle speed can be estimated without having to correct for mass changes using RLS. As the ***Q*** optimisation is carried out off-line using measured vehicle data, it is possible to run the estimator under more than one condition simultaneously for each potential value for ***Q***, the cost function is averaged across the different conditions to give J_{avg} (29). Measured data is recorded experimentally for motor torque, motor speed and vehicle speed, for both unloaded and loaded conditions at one speed level. This will double the computational required to evaluate each chromosome but will produce the optimal ***Q*** for both unloaded and loaded driving conditions, see Fig. 12. This could also be expanded for different driving speeds, torque levels and inclines, rather than just the 1500 rpm speed used in these tests.

Integrated absolute error (IAE) for motor speed (24) and vehicle speed (25) is calculated by working out the PU size of the absolute error, the integrated error is divide by the integrated measured speed, to give an IAE in the 0–1 range

$$\text{IAE}\omega_{\text{m}}(\text{PU}) = \frac{\sum_{k=1}^{n} ||\omega_{\text{m}}(k)| - |\hat{\omega}_{\text{m}}(k)||}{\sum_{k=1}^{n} |\omega_{\text{m}}(k)|} \tag{24}$$

$$\text{IAE}v_{\text{v}}(\text{PU}) = \frac{\sum_{k=1}^{n} ||v_{\text{v}}(k)| - |\hat{v}_{\text{v}}(k)||}{\sum_{k=1}^{n} |v_{\text{v}}(k)|} \tag{25}$$

Ideally the measurement noise variance (NV) would be reduced by the KF (NR noise reduction) for motor speed (26) and vehicle speed (27), the NV reduction (NVR) as a

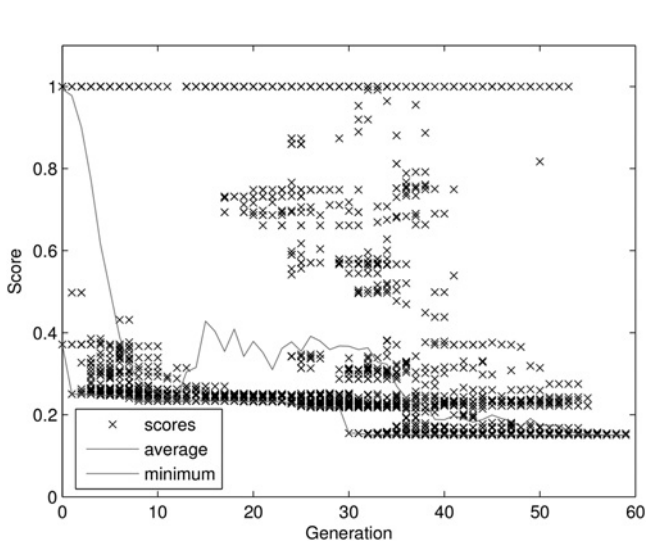

Fig. 13 *How the cost function improves with each iteration of the GA*

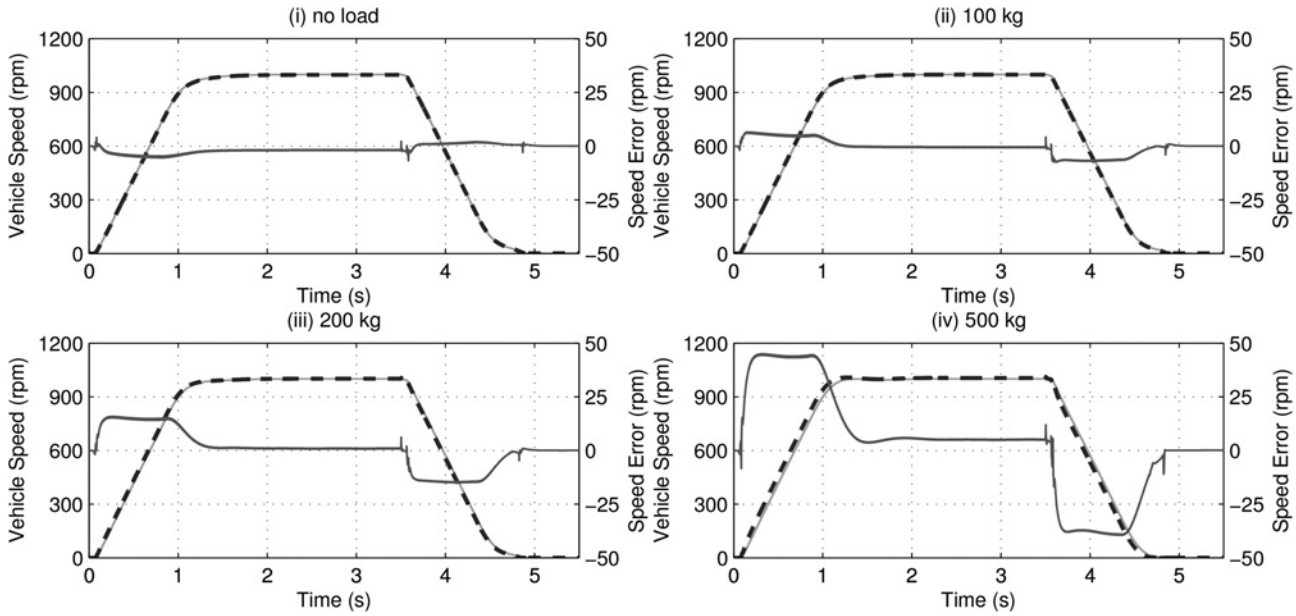

Fig. 14 *Simulation results of speed estimation (with GA tuned* ***Q****) at 1000 rpm with increasing load mass*
((i) 0, (ii) 100, (iii) 200, (iv) 500 kg)

© The Institution of Engineering and Technology 2013

doi: 10.1049/iet-est.2012.0027

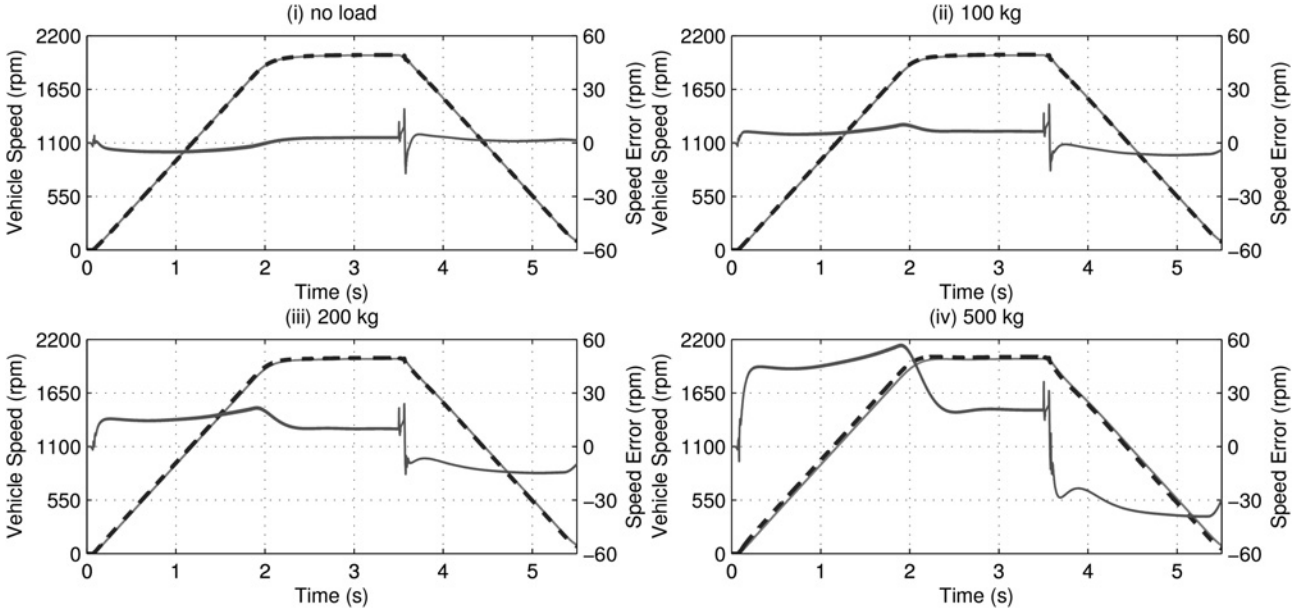

Fig. 15 *Simulation results of speed estimation (with GA tuned* $\boldsymbol{Q}$*) at 2000 rpm with increasing load mass*
((i) 0, (ii) 100, (iii) 200, (iv) 500 kg)

ratio (0 to 1) is calculated

$$\mathrm{NVR}\omega_{\mathrm{m}}(\mathrm{PU}) = \frac{\hat{N}V\omega_{\mathrm{m}}}{\mathrm{NV}\omega_{\mathrm{m}}} \tag{26}$$

$$\mathrm{NVR}v_{\mathrm{v}}(\mathrm{PU}) = \frac{\hat{N}Vv_{\mathrm{v}}}{\mathrm{NV}v_{\mathrm{v}}} \tag{27}$$

Cost function J for both unloaded or loaded conditions (28)

$$J_{\mathrm{unload/load}} = \frac{\mathrm{IAE}\omega_{\mathrm{m}} + \mathrm{IAE}v_{\mathrm{v}} + \mathrm{NVR}\omega_{\mathrm{m}} + \mathrm{NVR}v_{\mathrm{v}}}{4} \tag{28}$$

Overall cost function J_{avg} is the average cost function for both unloaded and loaded conditions (29)

$$J_{\mathrm{avg}} = \frac{J_{\mathrm{unload}} + J_{\mathrm{load}}}{2} \tag{29}$$

6.2 Tuning the process noise matrix with GA

GA is a search and optimisation algorithm that is used to find the best solution to a problem where the performance can be evaluated with a cost function. In this case finding the optimum value for the process noise matrix $\boldsymbol{Q}$ to minimise the integrated error of the estimated states and also reduce the noise content of these signals. The technique mimics natural evolution and is suitable for use on non-linear and noisy systems, as it can avoid local minima and is derivative free [13].

The basic operation of the algorithm follows these steps [13]:

- Initialise the population of 100 chromosomes with random possible solutions for $\boldsymbol{Q}$. These are initialised within a chosen predetermined range. As $\boldsymbol{Q}$ has five diagonal values, each chromosome contains five genes.
- Motor torque, motor speed and vehicle speed recorded from vehicle experiments are used to run the estimator off-line with each of the possible set of values for $\boldsymbol{Q}$. The Kalman gain $\boldsymbol{K}$ is calculated for the potential $\boldsymbol{Q}$ values, and then a fixed Kalman gain estimator is used. This then generates a performance indication of the estimator using a cost function – see Section 6.1.
- Selection is then carried out based upon the fitness result in the step above. The highest scoring (lowest cost function value) chromosomes are selected to for a pool of suitable candidates suitable for creating the next generation.
- In order to create the next generation, crossover with a probability ratio of 0.6, is performed on the pool of suitable parents above.
- Non-linear systems can have local minima that are not the most optimal solution. Mutation is therefore performed, with a probability ratio of 0.35, to ensure that the optimisation finds the overall most suitable values. It works by randomly changing a bit in one of the new chromosomes to change its value. Normally the mutation ratio would be quite low, but in this case it is higher because of there being many non-optimal minima.

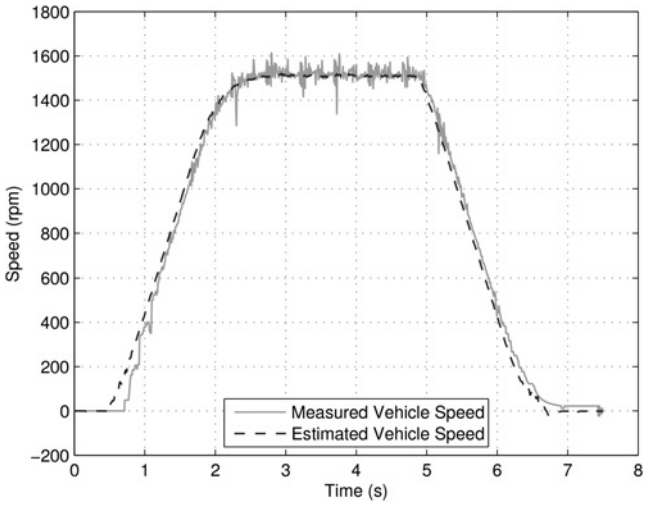

Fig. 16 *Experimental results of speed estimation (with GA tuned* $\boldsymbol{Q}$*) with 200 kg load mass and no mass estimation or correction*

© The Institution of Engineering and Technology 2013

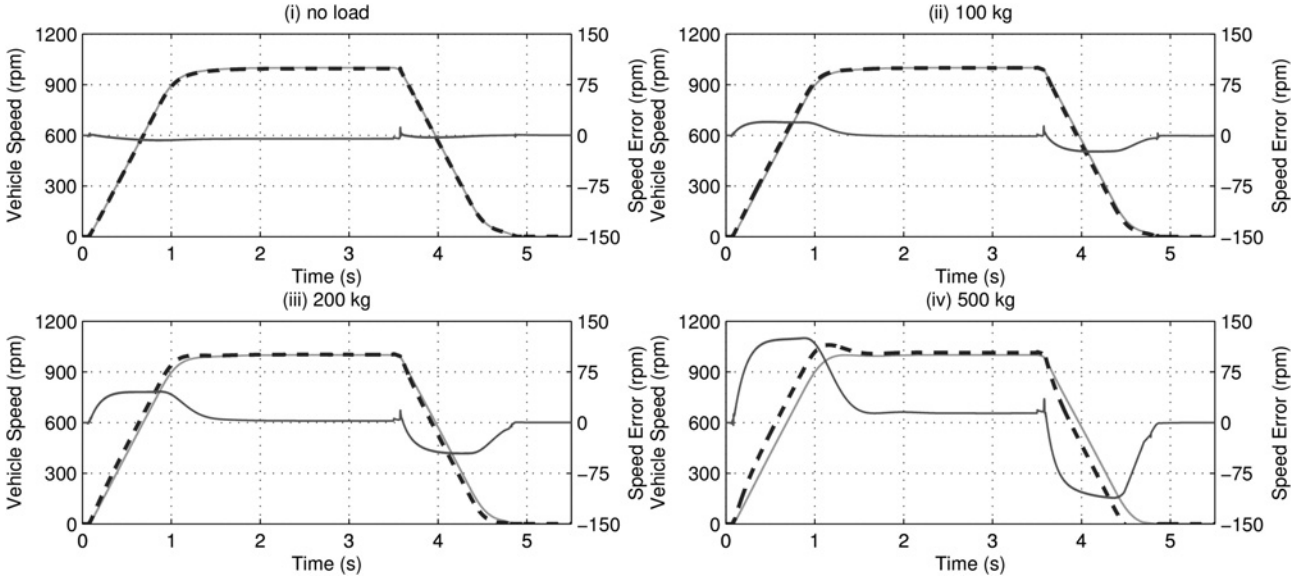

Fig. 17 *Simulation results of speed estimation (with LS tuned* $\boldsymbol{Q}$*) at 1000 rpm with increasing load mass*
((i) 0, (ii) 100, (iii) 200, (iv) 500 kg)

• The process is then repeated with the new set of possible $\boldsymbol{Q}$ values until either the maximum number of iterations is reached (100 iterations), or the desired performance is attained.

The GA algorithm in seen to mostly improve the average cost function performance at each generation step, see Fig. 13. In some cases, mutation leads to an increase in the average cost function, for example at 15 generations. However, ultimately this leads to the minimum cost function decreasing at around 30 generations. As otherwise the algorithm would converge and not reach the optimal point.

6.3 GA tuned estimator results

Now that the optimal value of $\boldsymbol{Q}$ has been found, the effect of mass changes on the estimator accuracy is tested. This is initially tested in simulation, then repeated with experimental data. With a speed demand of 1000 rpm, the speed estimation error is quite low, although increases with increasing load mass, see Fig. 14. When the speed is increased to 2000 rpm, the estimation error increases, although is still < 60 rpm with 500 kg load added; see Fig. 15. Measured vehicle speed is in solid green, estimated vehicle speed is dashed blue and the dotted red trace is the estimation error. Note the scaling of the speed error axis changes between figures.

Experimentally, the response has been tested without RLS mass estimation and compensation, but with a 200 kg load added; see Fig. 16.

The mass robustness of the estimator is greatly improved compared with the trial and error tuned $\boldsymbol{Q}$ without RLS mass compensation, Fig. 8. There is a small error during

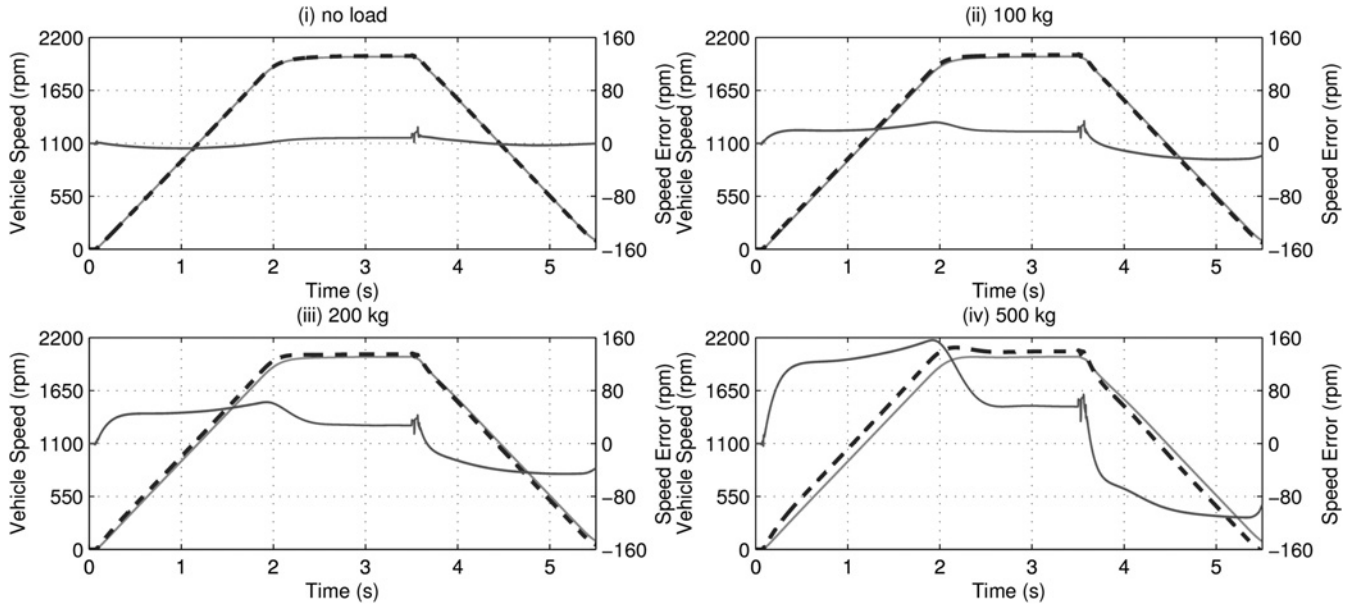

Fig. 18 *Simulation results of speed estimation (with LS tuned* $\boldsymbol{Q}$*) at 2000 rpm with increasing load mass*
((i) 0, (ii) 100, (iii) 200, (iv) 500 kg)

© The Institution of Engineering and Technology 2013

doi: 10.1049/iet-est.2012.0027

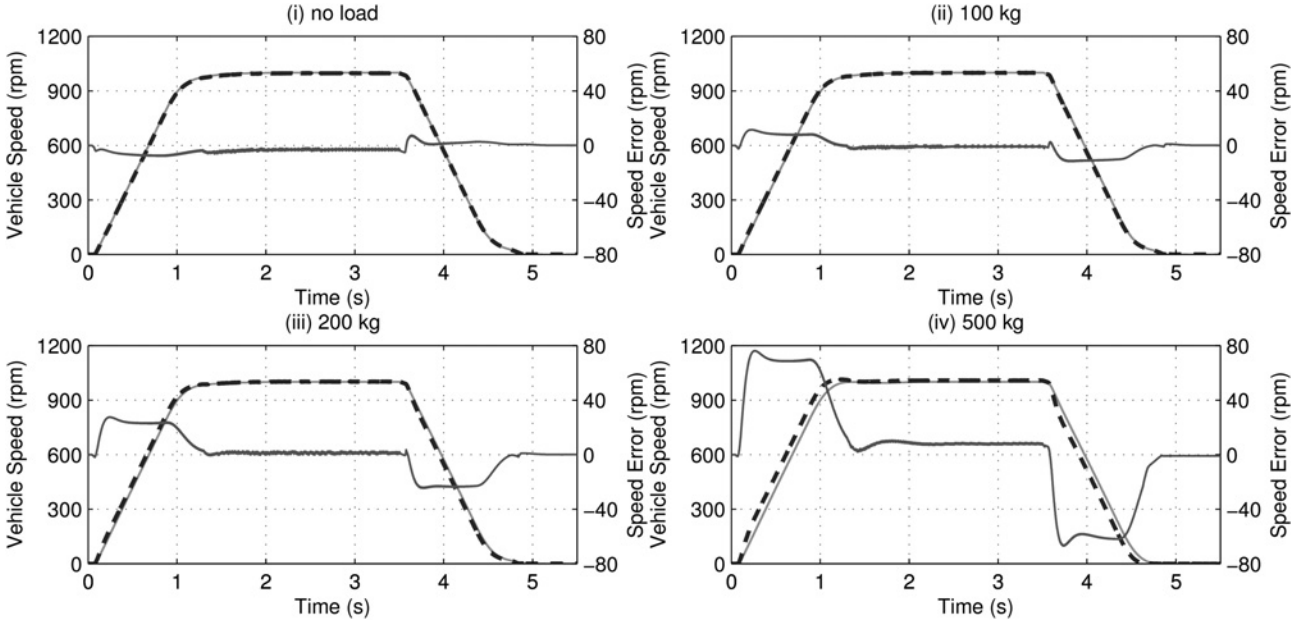

Fig. 19 *Simulation results of speed estimation (with MIN tuned* ***Q****) at 1000 rpm with increasing load mass*
((i) 0, (ii) 100, (iii) 200, (iv) 500 kg)

the acceleration but the performance is comparable with the trial and error tuned ***Q*** without a load mass change, Fig. 7, or better than with a load mass change and using the RLS compensator, Fig. 11.

6.4 Tuning the process noise matrix with other optimisation techniques

It is important to compare the performance of the GA method to other optimisation techniques. The same method as for the GA was used for analysing the estimator error; see Section 6.1. The issue with this is that there is no direct way of obtaining the differential of the cost function, an advantage of GA is that this is not required, but it is possible to approximate the differential of the cost function at each iteration to overcome this. Two alternative methods were compared: a non-linear least squares (LS)-based scheme (see Figs. 17 and 18), and a non-linear minimisation search (MIN) algorithm based on the Nelder–Mead method see Figs. 19 and 20.

At no load and with small mass changes the estimation is fairly accurate, but any large load added to the vehicle causes a large speed estimation error. The response in (17)–(20) was still better than the trial and error tuned Q 8.

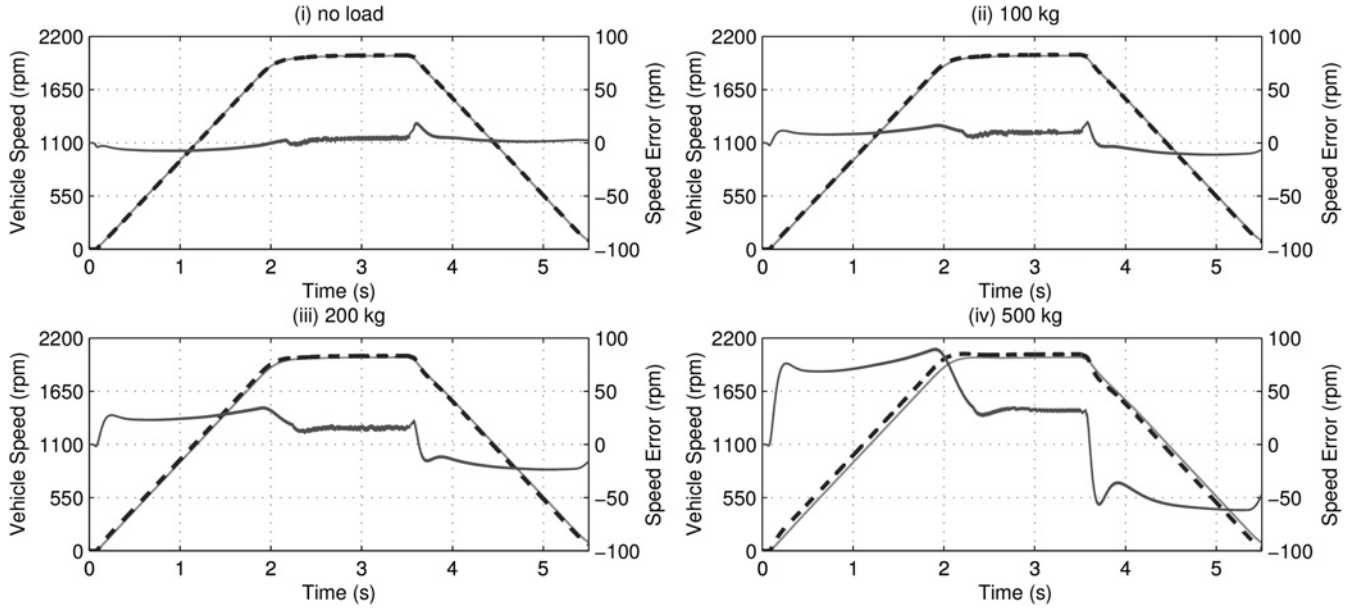

Fig. 20 *Simulation results of speed estimation (with MIN tuned* ***Q****) at 2000 rpm with increasing load mass*
((i) 0, (ii) 100, (iii) 200, (iv) 500 kg)

© The Institution of Engineering and Technology 2013

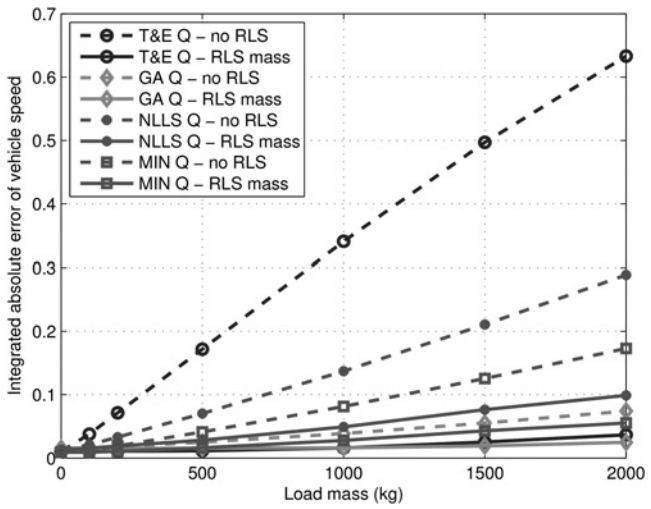

Fig. 21 *Graph showing how the $IAEv_v(PU)$ varies with mass*

6.5 Large mass changes – estimator robustness

It is possible for industrial EV applications to have more significant mass changes than the 200 kg experimentally tested, which is only equivalent to around 45% of the vehicles unloaded mass. The robustness of the estimator across larger mass changes has been tested in simulation as it is not possible to increase the load mass to much higher levels experimentally, Fig. 21. This is to see the limits of the estimation with both the trial and error $\boldsymbol{Q}$ and the GA tuned $\boldsymbol{Q}$, and also with and without the RLS mass estimator feedback for both cases.

The best performance over the large mass range was achieved using the GA tuned $\boldsymbol{Q}$, with and without the RLS mass compensation. The performance without mass estimation (for GA tuned $\boldsymbol{Q}$) was almost as good as for the other $\boldsymbol{Q}$ values with mass estimation. The trial and error tuned $\boldsymbol{Q}$ gave the worst response, for both with and without RLS mass compensation. The LS and the MIN algorithms gave acceptable response with the mass compensation, but poor without.

7 Conclusions

A solution has been proposed for improving the speed control of an EV by using a KF. It is computationally efficient as the Kalman gain is fixed and calculated off-line. Even in the case where the RLS mass estimate is used to correct the matrices within the KF, this only has to be done once after each time the vehicle moves away from stationary. This avoids having to use the EKF with all its extra on-line processing requirement.

It has been shown that it is possible to estimate the vehicle speed correctly when there is a significant change in the vehicle mass. Using a separate RLS mass estimator has been tested and also tuning the $\boldsymbol{Q}$ matrix to remove the requirement of using the RLS estimator. The importance of accurately tuning the process noise matrix $\boldsymbol{Q}$ has been shown and has successfully been carried out using a GA, which also takes into account the noise reduction of the KF.

The effect of gradients has not been considered and further work needs to be carried out to include the estimation of road incline. There is also the assumption that rolling resistance is proportional to mass changes, but for example, changes in tyre temperature can also change the rolling resistance coefficient C_0. The GA tuned estimator has been shown to be fairly robust to significant mass changes (2000 kg), >400% of the unloaded mass, so the effects of these assumptions should be quite small in comparison.

8 Acknowledgments

The authors acknowledge EPSRC and Sevcon for funding for this project.

9 References

1 Vahidi, H.P.A., Stefanopoulou, A.: 'Recursive least squares with forgetting for online estimation of vehicle mass and road grade: theory and experiments', *Veh. Syst. Dyn.*, 2005, **43**, (1), pp. 31–35
2 Hodgson, D., Mecrow, B.C., Gadoue, S.M., Slater, H.J., Barrass, P.G., Giaouris, D.: 'Accurate estimation of electric vehicle speed using kalman filtering in the presence of parameter variations'. Sixth IET Int. Conf., Power Electronics, Machines and Drives (PEMD 2012), March 2012, pp. 1–6
3 Berriri, M., Chevrel, P., Lefebvre, D.: 'Active damping of automotive powertrain oscillations by a partial torque compensator', *Control Eng. Pract.*, 2008, **16**, (7), pp. 874–883
4 Amann, N., Bocker, J., Prenner, F.: 'Active damping of drive train oscillations for an electrically driven vehicle', *IEEE/ASME Trans. Mechatronics*, 2004, **9**, (4), pp. 697–700
5 Thomsen, S., Fuchs, F.: 'Speed control of torsional drive systems with backlash'. 13th European Conf. Power Electronics and Applications, EPE'09. September 2009, pp. 1–10
6 Thomsen, S., Hoffmann, N., Fuchs, F.W.: 'Pi control, pi-based state space control, and model-based predictive control for drive systems with elastically coupled loads-a comparative study', *IEEE Trans. Ind. Electron.*, 2011, **58**, (8), pp. 3647–3657
7 Szabat, K., Orlowska-Kowalska, T.: 'Vibration suppression in a two-mass drive system using pi speed controller and additional feedbacks – comparative study', *IEEE Trans. Ind. Electron.*, 2007, **54**, (2), pp. 1193–1206
8 De Sousa, M.A.T.F., Caux, S., Fadel, M.: 'Design of robust controllers for pmsm drive fed with PWM inverter with inertia load variation', IEEE Internationl Symposium on Industrial Electronics, 2006, **1**, pp. 217–222
9 Szabat, K., Orlowska-Kowalska, T.: 'Performance improvement of industrial drives with mechanical elasticity using nonlinear adaptive Kalman filter', *IEEE Trans. Ind. Electron.*, 2008, **55**, (3), pp. 1075–1084
10 Kweon, T.-J., Hyun, D.-S.: 'High-performance speed control of electric machine using low-precision shaft encoder', *IEEE Trans. Power Electron.,* 1999, **14**, (5), pp. 838–849
11 Yan, S., Xu, D., Wang, G., Yang, M., Yu, Y., Gui, X.: 'Low speed control of pmac servo system based on reduced-order observer'. IEEE/RSJ Int. Conf. Intelligent Robots and Systems, October 2006, pp. 4886–4889
12 Karasalo, M., Hu, X.: 'An optimization approach to adaptive Kalman filtering', *Automatica*, 2011, **47**, (8), pp. 1785–1793
13 Gadoue, S., Giaouris, D., Finch, J.: 'Artificial intelligence-based speed control of DTC induction motor drives-A comparative study', *Electr. Power Syst. Res.*, 2009, **79**, (1), pp. 210–219
14 Lagerberg, A., Egardt, B.: 'Backlash estimation with application to automotive powertrains', *IEEE Trans. Control Syst. Technol.*, 2007, **15**, (3), pp. 483–493
15 Nordin, P.G.M., Galic, J.: 'New models for backlash and gear play', *Int. J. Adapt. Control Signal Process.*, 2006, **11**, pp. 49–63
16 Simon, D.: 'Optimal state estimation' (Wiley–Interscience, 2006)
17 Lingman, B.S.P.: 'Road slope and vehicle mass estimation using kalman filtering', *Veh. Syst. Dyn.*, 2002, **37**, pp. 12–23
18 Ohnishi, H., Ishii, J., Kayano, M., Katayama, H.: 'A study road slope estimation for automatic transmission control', *JSAE review, April* 2000, pp. 235–240
19 Ming, T., Lin, G., Deliang, L.: 'Sensorless permanent magnet synchronous motor drive using an optimized and normalized extended Kalman filter'. Int. Conf. Electrical Machines and Systems (ICEMS), August 2011, pp. 1–4
20 Szabat, K., Orlowska-Kowalska, T.: 'Performance improvement of industrial drives with mechanical elasticity using nonlinear adaptive Kalman filter', *IEEE Trans. Ind. Electron.,* 2008, **55**, (3), pp. 1075–1084

© The Institution of Engineering and Technology 2013

doi: 10.1049/iet-est.2012.0027